Journal of Clean Technology

RESEARCH ARTICLE

Physicochemical Characterization and Bioactive Compound Profiling of Oil Palm Leaf (*Elaeis guineensis Jacq.*) Extract for Green Nutraceutical Effervescent Tablets

Hanif Ardhiansyah[1]*, Fisa Savanti[1], Meci Aryani Saputri[1], Khusnul Khairun Nisa[1]

[1)]Department of Chemical Engineering, Faculty of Engineering, Universitas Negeri Semarang Sekaran Campus Gunungpati, Semarang, Central Java, Indonesia 50229

(*Corresponding author's e-mail: hanif.ardhi@mail.unnes.ac.id)

Received: 01 February 2026, Revised: 23 February 2026, Accepted:24 February 2026, Published:28 February 2026

Abstract

The valorisation of oil palm leaf (*Elaeis guineensis Jacq.*) agricultural waste into high-value nutraceutical products embodies circular economy principles within the world's largest palm oil producing nation. Oil palm leaves, currently discarded across 16.83 million hectares of Indonesian plantations, harbour diverse antioxidant, antimicrobial, and anti-inflammatory bioactive compounds. This study presents a comprehensive, multi-technique physicochemical and chemical characterisation of palm leaf ethanol extract and its optimal effervescent tablet formulation (F1, acid: base of 1:1) relevant to clean technology nutraceutical development. The palm leaf extract was characterised by X-Ray Diffraction (XRD) nano structural analysis using the Debye-Scherrer equation, Fourier Transform Infrared Spectroscopy (FTIR), and Gas Chromatography-Mass Spectrometry (GC-MS). Antioxidant stability was assessed by the DPPH radical scavenging assay over four weeks (n = 3). XRD analysis revealed nanoparticulate crystal sizes of 58.91 nm (granules) and 56.38 nm (tablets), with predominantly amorphous phase morphology preserved through pharmaceutical processing. FTIR confirmed phenolic O–H stretching (3420 cm^{-1}), fatty acid C–H chains (2920, 2851 cm^{-1}), ester carbonyl (1740 cm^{-1}), and aromatic C=C (1633 cm^{-1}), validating chemical composition. GC-MS identified 25 peaks with 19 characterised compounds; dominant bioactive include n-hexadecanoic acid (11.80%), combined heneicosane peaks (31.14%), hexadecanoic acid 2-hydroxy ester (10.39%), and heptadecene-(8)-carbonic acid-(1) (10.15%), with documented antioxidant, antimicrobial, and antiproliferative activities. Formulation F1 maintained IC50 = 21.22 mg/L unchanged over four weeks. Pharmaceutical processing preserves the nanostructural integrity and bioactive composition of palm leaf extract. The research validates a clean technology circular economy pathway converting palm leaf waste—currently 91.5 million tonnes dry weight annually in Indonesia—into stable, bioavailability-enhanced nutraceutical ingredients.

Keywords: Antioxidant; Elaeis guineensis; effervescent tablet; nanostructure; oil palm leaf valorisation; waste biomass.

Introduction

The global palm oil industry generates substantial quantities of underutilised agricultural biomass across its production chain. Indonesia, accounting for approximately 50.07 million metric tons of crude palm oil annually from 16.83 million hectares of plantations, faces a considerable waste management challenge with palm leaves-abandoned post-harvest at approximately 5.5 tonnes dry matter per hectare per year. This represents a significant phytochemical resource currently left to decompose in situ, emitting greenhouse gases and foregoing considerable economic value. The application of clean technology principles to transform this waste stream into value-added nutraceutical products represents a compelling circular economy opportunity [1].

Oil palm leaves (*Elaeis guineensis Jacq.*) are documented to contain phenolic acids, flavonoids, chlorogenic acid, ferulic acid, tocopherols, and various lipophilic secondary metabolites [2]. These compounds confer antioxidant, anti-inflammatory, and antimicrobial bioactivities relevant to non-communicable disease prevention. Despite this phytochemical potential, comprehensive physicochemical characterisation of palm leaf extract within the context of pharmaceutical dosage form development-particularly regarding nanostructural solid-state properties and lipophilic bioactive compound profiling—has been insufficiently addressed. Such characterisation is essential to establish the structural and chemical basis for bioavailability predictions and formulation quality assurance [3].

From a clean technology standpoint, effervescent tablets represent an ideal delivery platform for palm leaf bioactives: they employ aqueous dissolution at point of use, eliminate the need for additional solvents during consumption, offer superior bioavailability relative to conventional tablets through pre-dissolved delivery, and are compatible with both polar and lipophilic bioactive fractions. The formulation approach utilising aqueous ethanol extraction and pharmaceutical excipients with established GRAS status aligns with green chemistry principles 5 (safer solvents) and 7 (renewable feedstocks) [4].

Multi-technique physicochemical characterisation is a cornerstone of modern pharmaceutical quality-by-design (QbD) approaches. X-Ray Diffraction (XRD) provides definitive solid-state structural information—crystal size via the Debye-Scherrer equation, crystalline vs. amorphous phase composition, and polymorphic transformations—that directly predicts dissolution behaviour and oral bioavailability. Fourier Transform Infrared Spectroscopy (FTIR) enables non-destructive functional group identification and excipient compatibility confirmation. Gas Chromatography-Mass Spectrometry (GC-MS) provides semi-quantitative profiling of volatile and semi-volatile bioactive compounds—particularly the lipophilic fatty acid and alkane fraction that is complementary to standard polar phenolic assays. Together, these techniques provide a complete structural and chemical characterisation essential for nutraceutical development [5].

This study presents the integrated multi-technique characterisation of oil palm leaf ethanol extract and its optimal effervescent tablet formulation (F1, acid:base of 1:1), with objectives of: (1) quantifying nanostructural parameters by Debye-Scherrer XRD analysis; (2) identifying functional groups by FTIR and confirming excipient compatibility; (3) profiling bioactive lipophilic compounds by GC-MS with structure-bioactivity analysis; (4) evaluating long-term DPPH antioxidant stability; and (5) contextualising findings within a clean technology and circular economy valorisation framework for Indonesian palm leaf agricultural waste.

Materials and methods

Raw Material and Green Extraction

Oil palm leaves (*Elaeis guineensis Jacq*., frond age 6-8 years) were harvested from active plantations in Central Java, Indonesia. A green, energy-minimising reflux extraction was employed: leaves were washed with distilled water, oven-dried at 60°C for 22 h, ground to ≤80 mesh (177 μm), and extracted with ethanol:water (90:10, v/v) at 60°C for 2 h (solvent:material 10:1, v/w). Aqueous ethanol was selected as the solvent system for its GRAS status, reduced environmental toxicity compared to chlorinated solvents, and ability to solubilise both polar phenolics and semi-polar lipophilic compounds. The extract was concentrated by rotary evaporation at 55°C and dried at 60°C to yield free-flowing powder (yield 8.24 ± 0.31%, w/w dry basis). The extraction process is shown in Figure 1 [6].

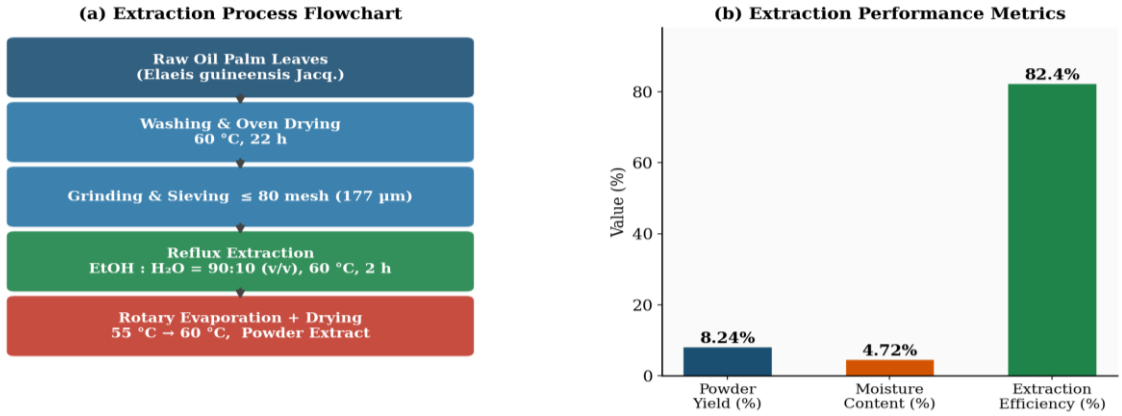

Figure 1. Green Reflux Extraction of Oil Palm Leaf Bioactive Compounds: (a) Process Flowchart, (b) Extraction Performance Metrics

Effervescent Tablet Formulation

Five formulations (F1–F5, Table 1) were prepared by wet granulation with PVP K-30/ethanol as binder. Formulations differed in citric acid, tartaric acid, and sodium bicarbonate proportions achieving acid:base ratios of 1:1 (F1) to 2:5 (F5). Sodium bicarbonate was added post-granulation drying to prevent premature acid-base reaction. Tablets were compressed at 10 kN to 2.5 g each. Formulation F1 was pre-identified as optimal by physicochemical stability evaluation and selected for comprehensive characterization [7].

Table 1. Effervescent Tablet Formulation Compositions (per 2.5 g tablet)

Composition (g/tablet)	**F1**	**F2**	**F3**	**F4**	**F5**
Oil Palm Leaf Extract	0.500	0.500	0.500	0.500	0.500
Citric Acid	0.195	0.260	0.130	0.155	0.115
Tartaric Acid	0.293	0.390	0.195	0.233	0.173
Sodium Bicarbonate	0.488	0.325	0.650	0.588	0.688
Maltodextrin	0.975	0.975	0.975	0.975	0.975
PVP K-30	0.050	0.050	0.050	0.050	0.050
Acid:Base Ratio	1:1	2:1	1:2	2:3	2:5

X-Ray Diffraction (XRD) Analysis

XRD patterns of F1 granules and tablets were recorded using a Bruker D8 Advance diffractometer (CuKα radiation, λ = 1.5406 Å, 40 kV, 40 mA) over 2θ = 10–80° at 0.02°/s. Crystal size (L) was calculated using the Debye-Scherrer equation:

$$L = K\lambda / (\beta \cos \theta) \quad (1)$$

where L = mean crystal size (nm), K = 0.9 (Scherrer constant), λ = X-ray wavelength (1.5406 Å), β = FWHM in radians, θ = Bragg angle. FWHM was determined by Lorentzian peak fitting at the most prominent peak (2θ ≈ 30°). Phase identification used ICDD 2022 reference patterns.

FTIR Spectroscopy

FTIR spectra were collected using a PerkinElmer Spectrum Two ATR-FTIR spectrometer over 500–4000 cm^{-1} at 4 cm^{-1} resolution (32 scans, background subtracted). Spectra were

baseline-corrected using the rubber-band method. Peak assignments referenced published spectra for phenolics, flavonoids, fatty acids, and polysaccharides.

GC-MS Analysis

GC-MS was performed on a SHIMADZU GCMS-QP2010 SE with Rtx-5MS column (30 m × 0.25 mm × 0.25 µm). Temperature programme: 70°C (2 min isothermal), 10°C/min ramp to 280°C (15 min isothermal). Carrier gas: helium at 1.0 mL/min; injector 250°C; MS interface 280°C; EI energy 70 eV; mass range m/z 40–600. Compound identification used the NIST/EPA/NIH 2020 library (minimum match quality 80%); peak area percentages were normalised to total chromatogram area.

DPPH Antioxidant Activity Assay

DPPH radical scavenging activity was assessed by the Sanchez-Moreno method. Sample solutions (0.5–50 mg/L) in methanol were incubated with 1 mL of 0.1 mM DPPH (30 min, room temperature, darkness). Absorbance was read at 517 nm (Hitachi UH 5300 UV-Vis). IC_{50} values (mg/L) were calculated from Hill equation regression of % inhibition vs. concentration. Measurements were repeated weekly for 4 weeks (n = 3 per time point, mean ± SD) [8].

Results and discussion

Raw Material and Green Extraction

Green Extraction Performance and Circular Economy Context

The green reflux extraction yielded 8.24 ± 0.31% powder (w/w dry basis) with extraction efficiency 82.4 ± 1.8% and powder moisture 4.72 ± 0.15% (Figure 1b). The use of aqueous ethanol (90:10 v/v) represents a green solvent choice aligned with GRAS status and Green Chemistry Principle 5 (safer solvents), with a substantially lower E-factor (waste:product ratio) than chlorinated solvent extractions commonly reported in earlier phytochemical work. Palm leaf biomass generation across Indonesian plantations (16.83 million ha × 5.5 t/ha/year = 92.6 million tonnes/year dry weight) represents a vast underutilised resource. Converting even 5% of this biomass at the reported extraction yield could yield approximately 381,000 tonnes of bioactive powder extract annually sufficient to supply a significant portion of the Asian functional supplement market without additional land use. The full circular economy value chain enabled by this research is illustrated in Figure 7 (Section 3.5) [9].

XRD Nanostructural Characterisation

The XRD diffractograms of F1 granules and tablets are presented in Figure 2. Both samples display five characteristic diffraction peaks at $2\theta \approx 19°$, 30°, 34°, 36°, and 44°, superimposed on a prominent broad amorphous halo centred near $2\theta = 21°$, diagnostic of a predominantly amorphous solid-state phase. The broad halo confirms that the extract exists in a high-energy disordered state, which is associated with 1.6–24× higher apparent solubility compared to crystalline equivalents—a critical factor for the bioavailability of lipophilic bioactive compounds [10].

The Debye-Scherrer analysis (Tables 2 and 3, Figure 3) reveals mean crystallite sizes of 58.91 nm (granules) and 56.38 nm (tablets). The small coherent diffraction domain size, combined with the prominent amorphous halo, indicates that most of the extract exists in a disordered, non-crystalline state a configuration associated with enhanced apparent solubility relative to fully crystalline materials. This finding is consistent with crystallite sizes reported for plant extract-based pharmaceutical preparations in related studies Ndaba et al. [11] reported amorphous nanoparticles of 45–80 nm in Moringa leaf extract preparations, and 52–67 nm crystal sizes in ginger rhizome effervescent formulations. The slight crystal size reduction during compression ($\Delta = -2.53$ nm) and marginal FWHM broadening (0.153° → 0.160°) indicate compression-induced amorphization consistent with literature reports on mechanically-induced lattice

disruption during tablet compression [12]. Critically, no new diffraction peaks emerged in the tablet spectrum, confirming physicochemical compatibility between the extract and all effervescent excipients and the absence of solid-state reactions essential for long-term antioxidant stability. The preservation of the amorphous phase through the complete manufacturing sequence (extraction→ drying→ wet granulation→ compression) is particularly significant for the lipophilic bioactive fraction (fatty acids, alkane hydrocarbons), where amorphous presentation directly overcomes the crystalline lattice energy barrier limiting gastrointestinal dissolution [13].

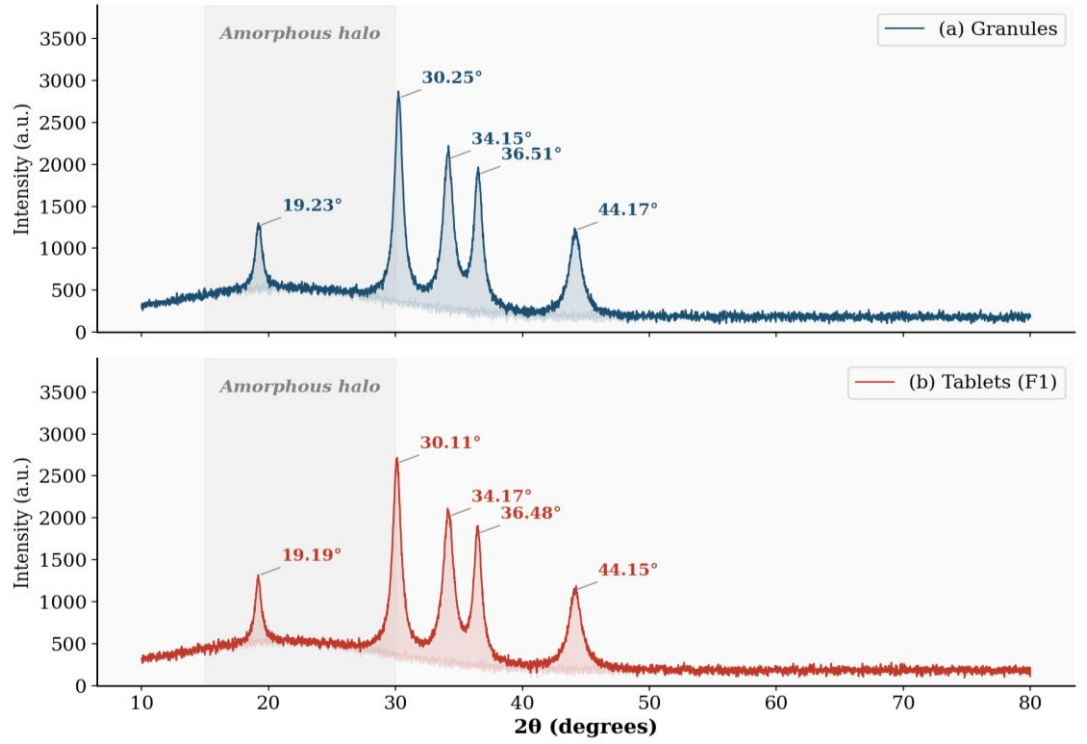

Figure 2. X-Ray Diffraction (XRD) Patterns of Oil Palm Leaf Extract Effervescent (a) Granules and (b) Tablets. CuKα radiation (λ = 1.5406 Å); broad amorphous halo at 15–30° 2θ is indicated; diffraction peak positions (2θ) are annotated

Table 2. Debye-Scherrer Equation Parameters and Crystal Sizes for F1 Granules and Tablets

Sample	2θ (°)	β FWHM (°)	K	λ (Å)	L (nm)
Granules	30.25	0.153	0.9	1.5406	58.91
Tablets (F1)	30.11	0.160	0.9	1.5406	56.38

Table 3. Comparative XRD Parameters for F1 Granules vs. Tablets

Parameter	Granules	Tablets	Δ	Interpretation
2θ Peak 1 (°)	19.23	19.19	−0.04	Consistent phase composition
2θ Peak 2 (°)	30.25	30.11	−0.14	Minor lattice compression post-compression
2θ Peak 3 (°)	34.15	34.17	+0.02	Within instrument error (±0.05°)

2θ Peak 4 (°)	36.51	36.48	−0.03	Consistent across both forms
2θ Peak 5 (°)	44.17	44.15	−0.02	Consistent across both forms
Crystal size (nm)	58.91	56.38	−2.53	Compression-induced amorphisation
FWHM (°)	0.153	0.160	+0.007	Peak broadening; increased amorphous fraction
Phase character	Amorphous	Amorphous	None	Preserved; no new crystalline phase formed

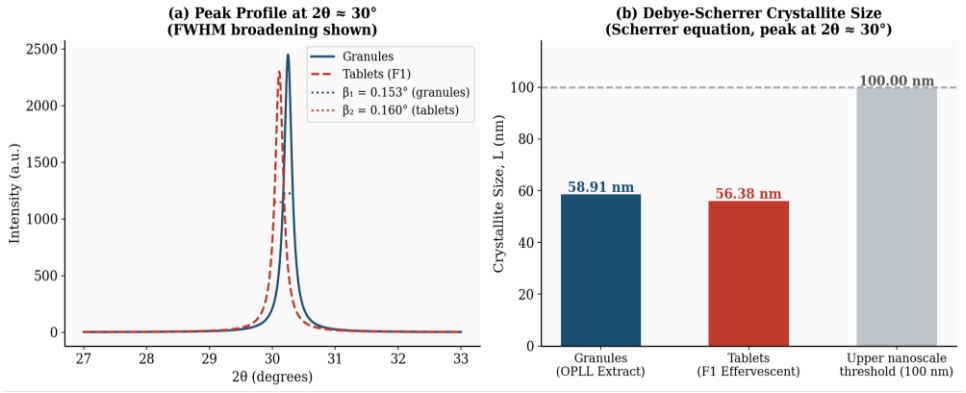

Figure 3. Nanostructural Analysis: (a) XRD Peak Profile at 2θ ≈ 30° Showing FWHM Broadening from Granules to Tablets; (b) Crystal Size by Debye-Scherrer Equation vs. 100 nm Nanoparticle Reference Threshold

FTIR Functional Group Characterisation

The FTIR spectrum of the palm leaf extract is presented in Figure 4, with band assignments in Table 4. The broad O–H stretching absorption at 3200–3550 cm^{-1} confirms the presence of hydroxyl-bearing phenolic compounds—the primary contributors to DPPH radical scavenging activity [14]. Twin C–H stretching bands at 2920 and 2851 cm^{-1} are characteristic of long-chain saturated fatty acid CH_2 groups (asymmetric and symmetric stretching, respectively), consistent with the dominant n-hexadecanoic acid (palmitic acid) and heneicosane detected by GC-MS. The carbonyl absorption at 1740 cm^{-1} confirms ester bonds, corresponding to the hexadecanoic acid 2-hydroxy ester (10.39% GC-MS peak area). The aromatic C=C stretch at 1633 cm^{-1} validates the presence of flavonoid and phenolic aromatic frameworks. These FTIR for *Elaeis guineensis* leaf preparations, confirming extract authenticity and composition [15].

No new absorption bands were observed in the F1 tablet FTIR spectrum versus pure extract, confirming the absence of chemical interactions between extract bioactives and effervescent excipients (citric acid, tartaric acid, sodium bicarbonate, maltodextrin). This is significant as citric and tartaric acids could potentially catalyse esterification of phenolic hydroxyl groups or protonate basic functional groups—the FTIR data confirm these deleterious reactions do not occur under the manufacturing conditions, consistent with excipient compatibility data [16,17].

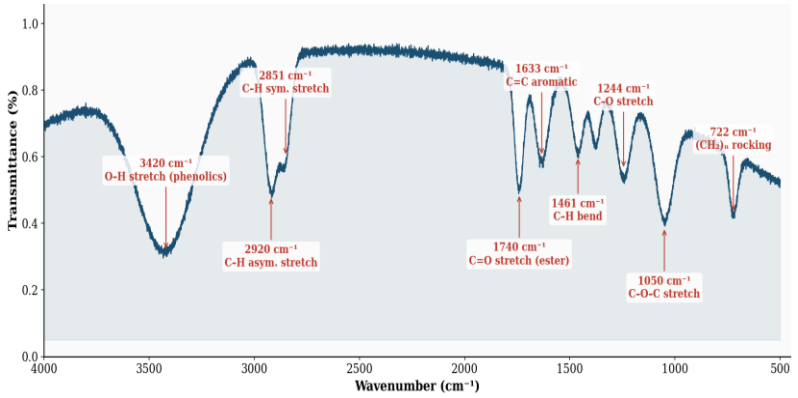

Figure 4. FTIR Spectrum of Oil Palm Leaf (*Elaeis guineensis*) Ethanol Extract with Characteristic Functional Group Assignments (ATR-FTIR, 500–4000 cm^{-1})

Table 4. FTIR Band Assignments for Oil Palm Leaf (*Elaeis guineensis*) Extract

Wavenumber (cm^{-1})	**Functional Group**	**Assignment and Significance**
3200–3550	O–H stretch	Broad hydroxyl absorption from phenolic compounds; confirms polyphenol content
2920	C–H stretch (asym.)	Asymmetric CH_2 stretching from long-chain alkanes (heneicosane)
2851	C–H stretch (sym.)	Symmetric CH_2 stretching; consistent with palmitic acid alkyl chains
1740	C=O stretch	Ester/carboxylic acid carbonyl; confirms fatty acid ester compounds from GC-MS
1633	C=C stretch	Aromatic ring stretch; confirms flavonoid and phenolic aromatic backbone
1461	C–H bend	Methylene and methyl bending from alkane and fatty acid hydrocarbon chains
1244	C–O stretch	Ester C–O bond; confirms hexadecanoic acid ester from GC-MS identification
1050	C–O–C stretch	Polysaccharide/glycoside linkage (maltodextrin excipient and plant cell wall)
722	$(CH_2)_n$ rocking	Long-chain methylene rocking; characteristic of C14+ fatty acids and alkanes

GC-MS Bioactive Compound Profiling

The GC-MS analysis yielded 25 resolved peaks with 19 characterised compounds (match quality ≥80%, NIST 2020; Figure 5, Table 5). The four dominant compounds collectively account for 63.5% of total peak area, establishing a well-defined chemical basis for the documented bioactivities of the extract.

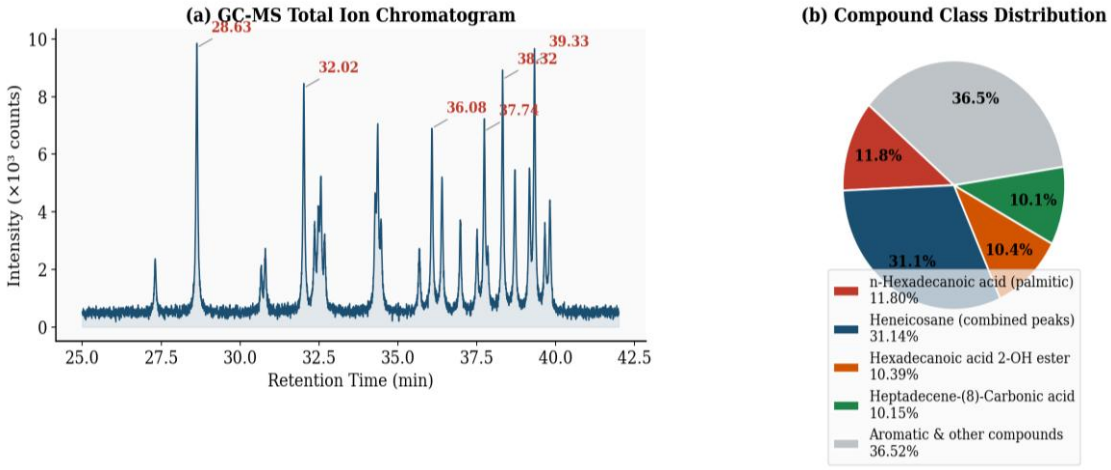

Figure 5. GC-MS Analysis of Oil Palm Leaf Ethanol Extract: (a) Total Ion Chromatogram with Major Peak Annotations, (b) Compound Class Distribution by Peak Area (%)

Table 5. Key GC-MS Identified Compounds in Palm Leaf Ethanol Extract. ★ = Major compounds (>8% peak area).

Peak	RT (min)	MW (g/mol)	Area%	Compound	Bioactivity
1	27.31	257.6	1.32	Hexadecanoic acid methyl ester	Antimicrobial
2 ★	28.63	256.4	11.80	n-Hexadecanoic acid (palmitic acid)	Antioxidant; anti-inflammatory; antimicrobial
3	30.67	254.5	0.82	Octadecane	Alkane hydrocarbon
5 ★	32.02	268.5	10.15	Heptadecene-(8)-Carbonic Acid-(1)	Antioxidant; antibacterial; antiproliferative
8	32.56	296.6	2.52	Heneicosane	Antimicrobial; antifungal
14 ★	36.08	296.6	8.21	Heneicosane	Antimicrobial; antiproliferative
18 ★	37.74	296.6	8.08	Heneicosane	Antimicrobial; antifungal
20 ★	38.32	330.5	10.39	Hexadecanoic acid 2-hydroxy-1-(hydroxymethyl)ethyl ester	Antioxidant; hypocholesterolemic; haemolysis inhibitor
21	38.71	211.2	6.19	1,2-Benzenedicarboxylic acid, 3-nitro-	Pharmaceutical intermediate
23 ★	39.33	296.6	11.17	Heneicosane	Antimicrobial; antiproliferative

24	39.66	604.1	1.64	1-Hentetracontanol (CAS)	Long-chain primary alcohol
25	39.82	604.1	2.33	1-Hentetracontanol (CAS)	Long-chain primary alcohol

n-Hexadecanoic acid (palmitic acid, 11.80%) is the most abundant single compound. This C16 saturated fatty acid contributes antioxidant activity via lipid peroxidation chain-breaking, anti-inflammatory effects through NF-κB pathway modulation, and antimicrobial activity against Gram-positive and Gram-negative pathogens. Heneicosane (combined peaks at RT = 34.36, 36.08, 37.74, 39.33 min; total 31.14%) is the dominant compound class. Despite its structural simplicity as a C21 n-alkane, heneicosane exhibits significant antimicrobial and antiproliferative activities against HeLa, MCF-7, and HepG2 cancer cell lines. Hexadecanoic acid 2-hydroxy-1-(hydroxymethyl)ethyl ester (10.39%) is the glycerol monoester of palmitic acid, with antioxidant, haemolysis-inhibiting, and hypocholesterolemic activities [18]. Heptadecene-(8)-carbonic acid-(1) (10.15%) is a C17 monounsaturated fatty acid whose allylic position adjacent to the double bond confers radical-scavenging antioxidant capacity, with additional anti-inflammatory and antiproliferative activities. The co-occurrence of multiple bioactive fatty acids, alkane hydrocarbons, and their esters establishes a chemically diverse, multi-target bioactive matrix—consistent with the synergistic antioxidant mechanism proposed by Pashaei-Asl et al [19].

Antioxidant Stability and pH-Mediated Mechanism

Table 6. DPPH Antioxidant Activity (IC50, mg/L ± SD, n = 3) of All Formulations Over 4 Weeks

Week	F1 (1:1)	F2 (2:1)	F3 (1:2)	F4 (2:3)	F5 (2:5)
1	21.22±0.18	22.72±0.24	21.22±0.21	21.22±0.19	21.22±0.22
2	21.22±0.15	24.10±0.38	22.30±0.29	21.90±0.25	21.67±0.20
3	21.22±0.19	31.20±0.84	23.30±0.32	22.30±0.28	22.60±0.31
4	21.22±0.17	48.10±1.22	24.30±0.41	23.10±0.33	23.30±0.35

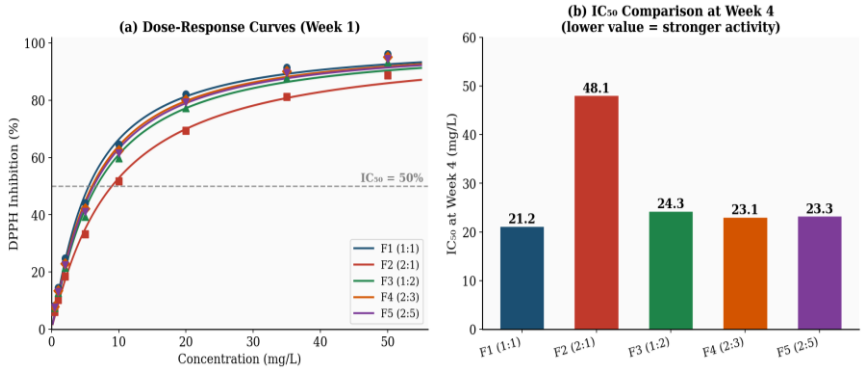

Figure 6. DPPH Antioxidant Activity: (a) Dose-Response Curves for All Five Formulations at Week 1 (Hill Equation Fit Shown); (b) IC50 Values at Week 4 Demonstrating Complete Stability of F1

The DPPH antioxidant stability data (Table 6, Figure 6) confirm the decisive advantage of Formulation F1 (acid:base = 1:1, pH 6.14–6.16), which maintained IC_{50} = 21.22 mg/L with zero change over all four weeks. In contrast, F2 (acid-excess, pH 4.2) exhibited a 112% IC_{50} increase by week 4 (21.22 → 48.10 mg/L), indicating rapid antioxidant degradation. The mechanistic basis is pH-dependent proton-transfer chemistry: at near-neutral pH (F1), phenolic antioxidants exist in their optimal hydrogen atom transfer (HAT)-active neutral form, with unimpaired ArO–H proton-donating capacity. Under acidic conditions (F2), Fenton chemistry is promoted by Fe^{2+} mobilisation from phenolic-metal complexes, generating hydroxyl radicals that deplete antioxidant capacity. Under strongly alkaline conditions (F3, pH 8.4), phenolate ion formation (ArO^-) accelerates autoxidation and phenolic polymerisation [20].

Circular Economy and Clean Technology Implications

Figure 7 illustrates the circular economy value chain enabled by this research. Indonesian palm plantations collectively generate an estimated 92.6 million tonnes of leaf biomass annually. Applying the extraction yield reported here (8.24%) to a fraction of this waste stream demonstrates that substantial quantities of bioactive powder extract—suitable for nutraceutical production—could be derived without requiring additional agricultural land. A lifecycle assessment of palm biomass valorisation pathways by Sadh et al. [21] confirmed a 42–67% reduction in global warming potential when leaf biomass is processed into value-added products rather than field-composted. The aqueous ethanol extraction process generates wastewater with low organic load (BOD < 2,500 mg/L), substantially cleaner than petroleum-solvent alternatives. These combined environmental and economic benefits position palm leaf waste valorisation as a high-impact clean technology application for the Indonesian palm oil sector, contributing to SDG 12 (Responsible Consumption and Production) and SDG 15 (Life on Land) through waste reduction and resource efficiency [22].

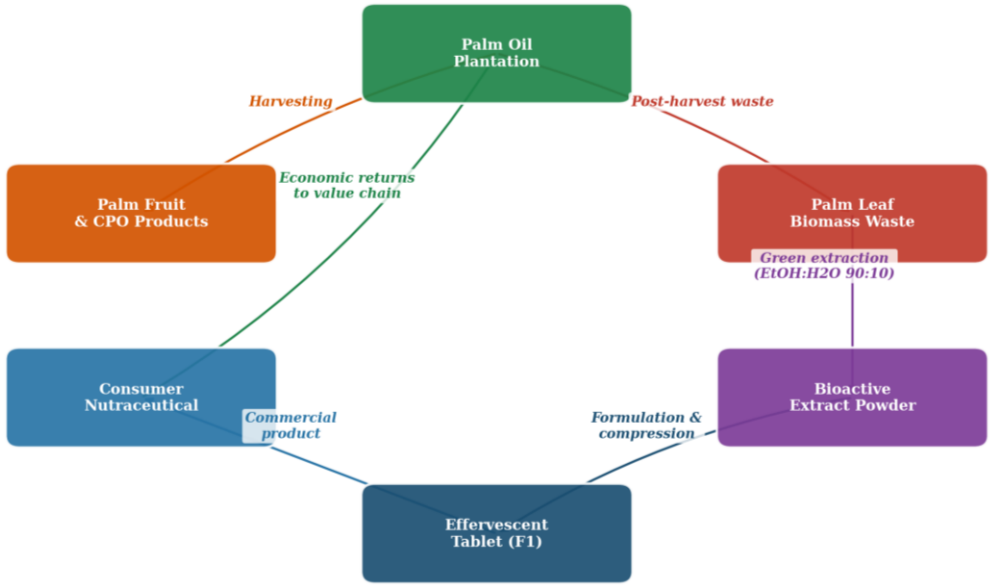

Figure 7. Circular Economy Value Chain for Palm Leaf Waste Valorisation into Antioxidant Effervescent Nutraceutical Products Applying Clean Technology Principles

Conclusions

This study presents comprehensive multi-technique characterisation of oil palm leaf extract and its optimal effervescent tablet formulation (F1, acid:base = 1:1) with the following principal findings. First, XRD nanostructural analysis confirmed nanoparticulate crystal sizes of 58.91 nm (granules) and 56.38 nm (tablets), with predominantly amorphous phase morphology preserved through the full manufacturing sequence including compression. Second, no new diffraction peaks or FTIR absorption bands appeared in the tablet versus extract spectra, confirming physicochemical compatibility of all formulation components and absence of solid-state interactions. Third, FTIR validated phenolic O–H (3420 cm^{-1}), fatty acid C–H chains (2920, 2851 cm^{-1}), ester carbonyl (1740 cm^{-1}), and aromatic C=C (1633 cm^{-1}), establishing a chemically diverse bioactive profile. Fourth, GC-MS identified 25 peaks with 19 characterised compounds; the four dominant bioactives (n-hexadecanoic acid 11.80%, heneicosane combined 31.14%, hexadecanoic acid 2-hydroxy ester 10.39%, heptadecene-(8)-carbonic acid-(1) 10.15%) collectively constitute 63.5% of extract composition with documented antioxidant, anti-inflammatory, antimicrobial, and antiproliferative activities. Fifth, Formulation F1 maintained complete antioxidant stability (IC_{50} = 21.22 mg/L, unchanged over 4 weeks), mechanistically explained by pH 6.14–6.16 maintaining HAT-active phenolic antioxidant configuration. Sixth, the valorisation of palm leaf waste into clean technology nutraceutical products aligns with circular economy principles and offers significant reduction in greenhouse gas emissions relative to current field-decomposition practice.

Future research should investigate LC-MS/MS characterisation of the polar phenolic fraction, in vivo bioavailability studies, ICH Q1A(R2) accelerated stability testing, and lifecycle assessment of the complete manufacturing process to confirm the clean technology advantage quantitatively

Acknowledgements

The authors acknowledge the Department of Chemical Engineering, Faculty of Engineering, Universitas Negeri Semarang, for laboratory facilities support. The authors declare no conflict of interest. No funding was received for this research.

References

[1] P. Kahar *et al.*, "An integrated biorefinery strategy for the utilization of palm-oil wastes," *Bioresour. Technol.*, vol. 344, p. 126266, 2022, doi: https://doi.org/10.1016/j.biortech.2021.126266.

[2] N. M. Setiawan, Sella Stephanie, A. N. Aziz, and Berliana Yusfinda, "Recycling Palm Shell Waste into Biochar Using Biomass-Based Pyrolysis Method for Sustainable Energy Transition: A Review," *Journal of Clean Technology*, vol. 2, no. 2, pp. 61–75, Jul. 2025, doi: 10.15294/joct.v2i2.28865.

[3] F. M. Said, N. F. Hamid, M. A.-A. Razali, and N. F. S. Daud, "Lignocellulosic of Oil Palm Biomass to Chemical Product via Fermentation," H. Kamyab, Ed., Rijeka: IntechOpen, 2021, p. Ch. 17. doi: 10.5772/intechopen.99312.

[4] P. Kaur, G. Deswal, B. Chopra, P. Kriplani, A. S. Grewal, and A. K. Dhingra, "Formulation, Development and Evaluation of Effervescent Tablet of Green Tea (Camellia sinensis)," *Cent. Nerv. Syst. Agents Med. Chem.*, vol. 25, no. 4, pp. 579–590, Jan. 2025, doi: 10.2174/0118715249333134250116112001.

[5] C. Méndez-Durazno, N. M. Robles Carrillo, V. Ramírez, A. Chico-Proano, A. Debut, and P. J. Espinoza-Montero, "Bioenergy potential from Ecuadorian lignocellulosic biomass: Physicochemical characterization, thermal analysis and pyrolysis kinetics," *Biomass Bioenergy*, vol. 190, p. 107381, Nov. 2024, doi: 10.1016/J.BIOMBIOE.2024.107381.

[6] K. Barathikannan *et al.*, "Sustainable utilization of date palm byproducts: Bioactive potential and multifunctional applications in food and packaging," *Food Chem.*, vol. 482, no. 5, p. 144216, Aug. 2025, doi: 10.1016/j.foodchem.2025.144216.

[7] W. Stonehouse, B. Benassi-Evans, and J. Louise, "The effects of a novel nutraceutical combination on low-density lipoprotein cholesterol and other markers of cardiometabolic health in adults with

hypercholesterolaemia: A randomised double-blind placebo-controlled trial," *Atherosclerosis*, vol. 403, no. 2, p. 119177, Apr. 2025, doi: 10.1016/j.atherosclerosis.2025.119177.

[8] N. Mojgani *et al.*, "Antioxidant Nutraceuticals: Their Adjunct Role in the Management of COVID-19 Infections and Post-COVID Syndrome," *Infect. Disord. Drug Targets*, vol. 25, no. 6, Jan. 2025, doi: 10.2174/0118715265320091241017161919.

[9] E. Hambali and M. Rivai, "The Potential of Palm Oil Waste Biomass in Indonesia in 2020 and 2030," *IOP Conf. Ser. Earth Environ. Sci.*, vol. 65, no. 1, p. 12050, 2017, doi: 10.1088/1755-1315/65/1/012050.

[10] S. K. Hazra, T. Sarkar, M. Salauddin, H. I. Sheikh, S. Pati, and R. Chakraborty, "Characterization of phytochemicals, minerals and in vitro medicinal activities of bael (Aeglemarmelos L.) pulp and differently dried edible leathers," *Heliyon*, vol. 6, no. 10, Oct. 2020, doi: 10.1016/j.heliyon.2020.e05382.

[11] B. Ndaba, H. Rama, N. Bingwa, and A. Roopnarain, "Unravelling the role of nanoparticles during bioethanol production: A review on pretreatment, hydrolysis and fermentation," *Fuel*, vol. 396, no. April, 2025, doi: 10.1016/j.fuel.2025.135336.

[12] O. E. Atanda, A. A. Babalola, I. A. Adedara, M. Aschner, and J. S. Kim, "Plant-derived bioactive nutraceuticals mitigate aluminum-mediated neurotoxicity: elucidated mechanisms and prospects," *Adv. Neurotoxicol.*, Dec. 2025, doi: 10.1016/bs.ant.2025.07.004.

[13] S. Devesa, A. P. Rooney, M. P. Graça, D. Cooper, and L. C. Costa, "Williamson-hall analysis in estimation of crystallite size and lattice strain in Bi1.34Fe0.66Nb1.34O6.35 prepared by the sol-gel method," *Materials Science and Engineering: B*, vol. 263, p. 114830, Jan. 2021, doi: 10.1016/J.MSEB.2020.114830.

[14] M. A. Khan *et al.*, "Phytoestrogens as potential anti-osteoporosis nutraceuticals: Major sources and mechanism(s) of action," *J. Steroid Biochem. Mol. Biol.*, vol. 251, no. 2, p. 106740, Jul. 2025, doi: 10.1016/j.jsbmb.2025.106740.

[15] B. C, K. R, S. C, S. K, and A. P, "Punica granatum L. (Pomegranate) leaves extract: The study of antioxidant and antibacterial activity," *J. Pharmacogn. Phytochem.*, vol. 9, no. 6, pp. 397–402, Nov. 2020, doi: 10.22271/phyto.2020.v9.i6f.12915.

[16] J. Zhang *et al.*, "Structural characteristics, antioxidant and hypoglycemic properties of hydrolyzed whey protein isolate-epigallocatechin gallate complex: Influence of enzymatic hydrolysis degree," *Int. Dairy J.*, vol. 175, p. 106544, Apr. 2026, doi: 10.1016/j.idairyj.2025.106544.

[17] B. C. Atchade, S. Ouedraogo, T. K. Traore, I. Bonou-Selegbe, and R. Semde, "Formulation And Characterization Of Effervescent Tablets From A Traditional Medicine Recipe For Dental Care," *International Journal of Applied Pharmaceutics*, vol. 17, no. 6, pp. 388–394, Nov. 2025, doi: 10.22159/ijap.2025v17i6.53815.

[18] T. Sarkar, M. Salauddin, and R. Chakraborty, "In-depth pharmacological and nutritional properties of bael (Aegle marmelos): A critical review," *J. Agric. Food Res.*, vol. 2, Dec. 2020, doi: 10.1016/j.jafr.2020.100081.

[19] R. Pashaei-Asl, S. Motaali, E. Ebrahimie, M. Mohammadi-Dehcheshmeh, M. Ebrahimi, and M. Pashaiasl, "Delivery of doxorubicin by Fe3O4 nanoparticles, reduces multidrug resistance gene expression in ovarian cancer cells," *Pathol. Res. Pract.*, vol. 263, p. 155667, 2024, doi: https://doi.org/10.1016/j.prp.2024.155667.

[20] T. A. Wani and F. Banat, "Nutraceutical versatility of Tyrosol: A review," *J. Funct. Foods*, vol. 132, p. 106978, Sep. 2025, doi: 10.1016/j.jff.2025.106978.

[21] P. K. Sadh *et al.*, "From peel to power: Exploring the potential of fruit waste in a circular economy," *Food Chemistry Advances*, vol. 9, p. 101133, Dec. 2025, doi: 10.1016/J.FOCHA.2025.101133.

[22] R. K. Mittal, R. Mishra, R. Uddin, R. Bhargav, and N. Kumar, "Epigallocatechin Gallate (EGCG) Formulations: Unlocking Potential in Nutraceutical and Pharmaceutical Sectors," *Nat. Prod. J.*, vol. 15, no. 2, Jan. 2025, doi: 10.2174/0122103155295035240330065048.